JACS
JOURNAL OF THE AMERICAN CHEMICAL SOCIETY

ARTICLE

pubs.acs.org/JACS

Proton-Coupled Electron Transfer Reactions at a Heme-Propionate in an Iron-Protoporphyrin-IX Model Compound

Jeffrey J. Warren*,† and James M. Mayer*,‡

†Beckman Institute, California Institute of Technology, MC 139-74, Pasadena, California 91125-0001, United States

‡Department of Chemistry, University of Washington, Box 351700, Seattle, Washington 98195-1700, United States

Supporting Information

ABSTRACT: A heme model system has been developed in which the heme-propionate is the only proton donating/accepting site, using protoporphyrin IX-monomethyl esters ($PPIX_{MME}$) and *N*-methylimidazole (MeIm). Proton-coupled electron transfer (PCET) reactions of these model compounds have been examined in acetonitrile solvent. $(PPIX_{MME})Fe^{III}(MeIm)_2$-propionate ($\mathbf{Fe^{III}}\sim\mathbf{CO_2}$) is readily reduced by the ascorbate derivative 5,6-isopropylidine ascorbate to give $(PPIX_{MME})Fe^{II}(MeIm)_2$-propionic acid ($\mathbf{Fe^{II}}\sim\mathbf{CO_2H}$). An excess of the hydroxylamine TEMPOH or of hydroquinone similarly reduces $\mathbf{Fe^{III}}\sim\mathbf{CO_2}$, and TEMPO and benzoquinone oxidize $\mathbf{Fe^{II}}\sim\mathbf{CO_2H}$ to return to $\mathbf{Fe^{III}}\sim\mathbf{CO_2}$. The measured equilibrium constants, and the determined pK_a and $E_{1/2}$ values, indicate that $\mathbf{Fe^{II}}\sim\mathbf{CO_2H}$ has an effective bond dissociation free energy (BDFE) of 67.8 ± 0.6 kcal mol^{-1}. In these PPIX models, electron transfer occurs at the iron center and proton transfer occurs at the remote heme propionate. According to thermochemical and other arguments, the TEMPOH reaction occurs by *concerted* proton−electron transfer (CPET), and a similar pathway is indicated for the ascorbate derivative. Based on these results, heme propionates should be considered as potential key components of PCET/CPET active sites in heme proteins.

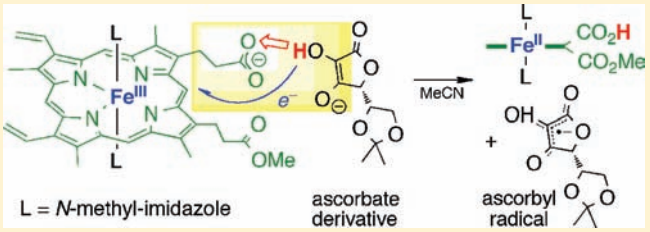

1. INTRODUCTION

Many reactions commonly understood as electron transfer reactions involve protons as well as electrons. These proton-coupled electron transfer (PCET) reactions are central to a wide range of chemical and biochemical processes, from biosynthetic pathways to energy transduction.[1] Heme enzymes are ubiquitous in biology and frequently utilize PCET. For instance, the catalytic cycles of peroxidases and related enzymes involve the addition of H^+ and e^- to the reactive ferryl (Fe=O) group to return to the Fe(III) resting state.[2] Many of the substrates of heme enzymes react with the transfer of both H^+ and e^-, including dioxygen, C−H bonds, hydroquinones, and ascorbate.[3] Ascorbate ($AscH^-$) oxidation occurs by loss of $1e^-$ and $1H^+$ to give the semidehydroascorbyl radical $Asc^{\bullet-}$, as in its oxidation by the bis(histidine)-ligated heme in cytochrome b_{561}.[4] Under physiological conditions, ascorbate oxidation has been shown to occur by transfer of $1e^- + 1H^+$ in a single kinetic step, termed concerted proton−electron transfer (CPET).[4,5] CPET is a common mechanism for many of these substrates because of the high energy of the intermediates that would be formed on transfer of the electron alone or the proton alone.[3]

In ascorbate peroxidase (APX), and in other heme enzymes,[6,7] the substrate is located distant from the iron. Therefore the proton (H^+) lost upon $AscH^-$ oxidation is transferred to a site other than the ferryl.[8,9] This contrasts with the typical mechanism of ferryl active sites, such as the oxidations of unactivated C−H bonds by cytochromes P450. In the P450 catalytic cycle, the RH substrate transfers a proton to the oxo group and an electron to a hole mostly on the heme.[2] This mechanism is typically called hydrogen atom transfer (HAT), despite the separation of the proton and electron in the product. X-ray crystal structures of APX show that ascorbate binds in a pocket next to the heme, where it is a hydrogen bond donor to the heme propionate (Figure 1).[8,9] The studies reported here indicate that the propionate is playing the proton-accepting role in this PCET reaction, as first suggested in a recent computational study.[9] A similar situation may occur in quinol:fumarate reductase (QFR), the terminal enzyme in fumarate respiration. Transmembrane electron transfer (ET) in QFR is coupled to proton transfer, potentially by coupling ET to/from the heme-iron to proton transfer between a heme propionate and an essential glutamate residue in the proton transfer "e-pathway."[7] Heme-propionates have also been implicated in the ET/proton pumping action of cytochrome *c* oxidase.[10] In related work, Das and Medhi have shown that small molecule iron-protoporphyrin IX complexes have reduction potentials that are dependent upon the protonation state of the propionates.[11]

Described here is the first well-characterized small-molecule model of PCET or CPET reactivity involving the heme-propionate as the essential base. In these PCET reactions, redox change occurs at the iron and proton transfer occurs at the propionate.

Received: June 25, 2010
Published: April 27, 2011

dx.doi.org/10.1021/ja201663p | *J. Am. Chem. Soc.* 2011, 133, 8544–8551

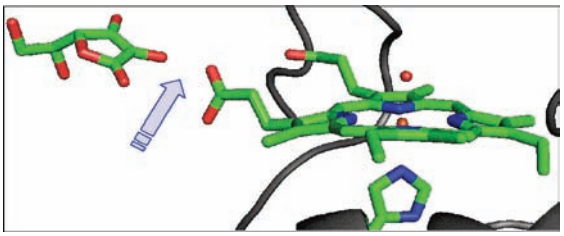

Figure 1. A portion of the X-ray crystal structure of APX,[8a] with the ascorbate-to-propionate hydrogen bond indicated by the arrow.[12].

One example is shown to occur by concerted transfer of e^- and H^+ (CPET), despite the large separation between the propionate and the iron. These studies mimic some of the biological PCET reactions above. They also complement ultrafast kinetic studies of PCET reactions of nickel and zinc purpurins (porphyrin derivatives) in which photoinduced electron transfer is accompanied by proton transfer from a conjugated amidinium group to a hydrogen-bonded naphthalenediimide acceptor.[13]

2. RESULTS

2.1. Synthesis and Characterization of Compounds. In order to have a model system in which there is only one site for acid/base reactivity, we have prepared iron complexes with the monomethyl ester of protoporphyrin IX ($PPIX_{MME}$) and *N*-methylimidazole (MeIm).[14] This system is related to our recently described iron-porphyrin models in which a ligated imidazolate is the proton-accepting site.[15] $Fe^{III}(PPIX_{MME})Cl$ was synthesized as reported from hemin chloride and MeOH/H_2SO_4 in THF.[16] Subsequent treatment with AgOTf in THF, and then MeIm, yields $[Fe^{III}(PPIX_{MME})(MeIm)_2]OTf$ (abbreviated $\mathbf{Fe^{III}{\sim}CO_2H^+}$), which has been isolated and characterized. ^1H NMR spectra in CD_3CN show that $\mathbf{Fe^{III}{\sim}CO_2H^+}$ is a 1:1 mixture of isomers that differ only in which propionate was esterified (the full spectrum is given in the Supporting Information). These isomers have identical kinetic and thermochemical properties to the extent that we can determine.

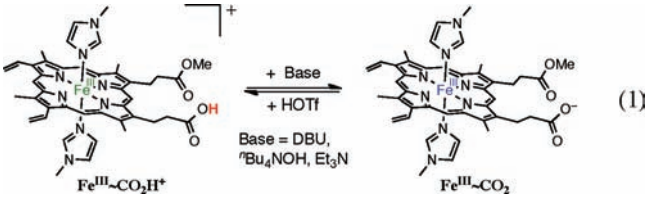

(1)

Spectrophotometric titrations of 2×10^{-5} M $\mathbf{Fe^{III}{\sim}CO_2H^+}$ with the bases DBU (1,8-diazabicyclo(5.4.0)undec-7-ene) or ^{n}Bu$_4$NOH (1 M in MeOH), show a decrease in the intensity of the Q-band centered at 533 nm up to one equivalent of base. The spectral changes are reversible with 1 equivalent of triflic acid (HOTf), consistent with production of the deprotonated species $\mathbf{Fe^{III}{\sim}CO_2}$ (eq 1; only one methyl-ester isomer is shown). Visible spectra showing the porphyrin Q-bands for these species, and for the ferrous derivative $\mathbf{Fe^{III}{\sim}CO_2H^+}$, are given in Figure 2.[17] Titration with the base Et_3N gives $pK_a(\mathbf{Fe^{III}{\sim}CO_2H^+}) = 21.1 \pm 0.3$. These measurements, and all of the measurements reported here, were done in MeCN containing 5 mM MeIm and 0.1 M ^{n}Bu$_4$NPF$_6$. The added MeIm ensures that all of the complexes have six-coordinate iron centers, as previously described.[15] The ^{n}Bu$_4$NPF$_6$ is added to give the same solution conditions as those

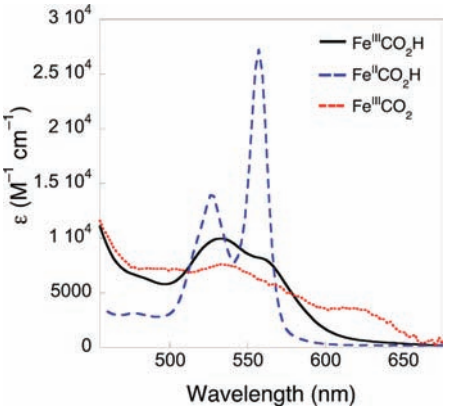

Figure 2. Visible spectra of the Q-bands of $\mathbf{Fe^{III}{\sim}CO_2H^+}$ (black), $\mathbf{Fe^{II}{\sim}CO_2H}$ (blue), and $\mathbf{Fe^{III}{\sim}CO_2}$ (red).

Scheme 1. Thermochemistry of Fe(PPIX$_{MME}$) System in MeCN

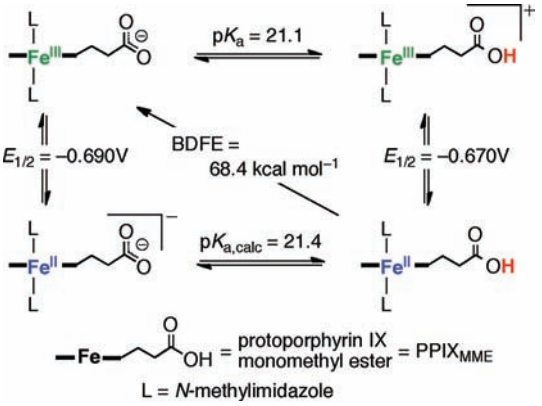

used for the electrochemical studies; when constructing thermochemical cycles such as Scheme 1 it is important to keep the measurement conditions as similar as possible. Et_3N titrations were done either working quickly with a standard spectrophotometer or, more conveniently, with stopped-flow mixing, to avoid the slow precipitation of $\mathbf{Fe^{III}{\sim}CO_2}$ that occurs (over 10−20 min for $(1-5) \times 10^{-5}$ M solutions). This could be due to formation of a dimeric species similar to β-hemeetin.[18]

Adding 1 equiv of cobaltocene to a solution of $\mathbf{Fe^{III}{\sim}CO_2H}$ causes the appearance of new Q-bands, indicating the production of the iron(II) complex $Fe^{II}(PPIX_{MME})(MeIm)_2$ ($\mathbf{Fe^{II}{\sim}CO_2H}$). The λ_{max} and ε are in agreement with similar model complexes[19] and with ferrous, bis(histidine)-ligated cytochrome b_5.[20] Cyclic voltammograms of $\mathbf{Fe^{III}{\sim}CO_2H^+}$ in MeCN with 5 mM MeIm and 0.1 M ^{n}Bu$_4$NPF$_6$ show a reversible wave at -0.670 ± 0.010 V versus $Cp_2Fe^{+/0}$. Addition of 1 equiv of ^{n}Bu$_4$NOH causes a small shift of the wave to -0.690 ± 0.010 V versus $Cp_2Fe^{+/0}$, which is reversed with 1 equiv of HOTf. The redox potentials, and the small shift in $E_{1/2}$ upon deprotonation of the propionate, were also confirmed by equilibration with decamethylferrocene (Cp^*_2Fe) (see Supporting Information).

The pK_a and redox potential results are summarized in Scheme 1, which provides a thermochemical map of this system.[3] $\mathbf{Fe^{III}{\sim}CO_2}$ and $\mathbf{Fe^{II}{\sim}CO_2H}$ differ by $H^+ + e^-$ or, equivalently, $H^\bullet$. The free energy for $\mathbf{Fe^{II}{\sim}CO_2H \rightarrow Fe^{III}{\sim}CO_2} + H^\bullet$ is given

dx.doi.org/10.1021/ja201663p |*J. Am. Chem. Soc.* 2011, 133, 8544–8551

by $1.37pK_a + 23.06E_{1/2} + C_G = 68.4 \pm 1.2$ kcal mol^{-1}.[21] This is analogous to a homolytic bond dissociation free energy (BDFE) although there is no formal bond homolysis of $\mathbf{Fe^{II}{\sim}CO_2H}$, since the proton is heterolytically cleaved from the carboxylate and the electron comes from the iron center. A similar analysis has been applied to reagents such as ferrocene-carboxylate, which has been used as a net H-atom donor,[22] and to PCET reactions that employ separate reductant and acid reagents (or oxidant and base reagents).[3,23] From a thermodynamic perspective, all of these "BDFEs" are equivalent.[3]

2.2. PCET Reactivity of $\mathbf{Fe^{II/III}{\sim}CO_2(H)}$. *2.2.1. Reactions with 5,6-Isopropylidene Ascorbate.* The oxidized, deprotonated complex $\mathbf{Fe^{III}{\sim}CO_2}$ reacts very rapidly with 5,6-isopropylidene ascorbate (*i*AscH$^-$) to give a ferrous porphyrin $\mathbf{Fe^{II}{\sim}CO_2H}$ and the corresponding ascorbyl radical *i*Asc$^{\bullet-}$ (eq 2). *i*AscH$^-$ is an MeCN soluble analog of ascorbate, with thermochemical properties similar to those of ascorbate; the formation of the *i*Asc$^{\bullet-}$ radical was confirmed by EPR (Supporting Information, Figure S7).[24] Optical spectra of reaction mixtures show the quantitative formation of a ferrous porphyrin but do not distinguish between its protonated and deprotonated forms ($\mathbf{Fe^{II}{\sim}CO_2H}$ vs $\mathbf{Fe^{II}{\sim}CO_2^-}$, see Experimental Section). Keeping track of the proton is often a challenge in PCET systems where the redox and acid/base sites are quite separated.[25] The formation of the protonated ferrous derivative, as shown in eq 2, is indicated by the stoichiometry of the reaction and by experiments discussed below.

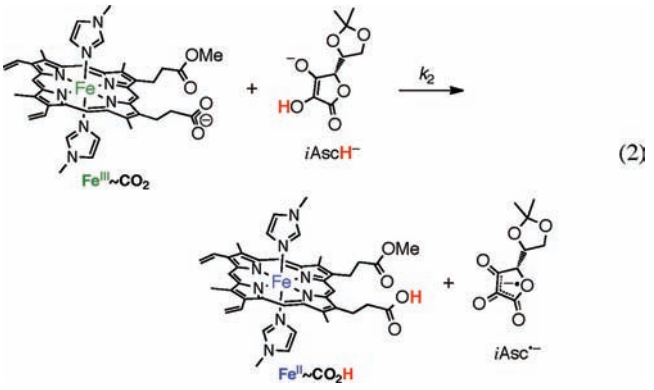

(2)

Stopped-flow kinetic measurements under pseudo-first-order conditions of excess *i*AscH$^-$ indicate that reaction 2 is first-order in both $\mathbf{Fe^{III}{\sim}CO_2}$ and *i*AscH$^-$, with $k_2 = (7.0 \pm 0.4) \times 10^4$ M^{-1} s^{-1} at 298 K. Similar measurements with *i*AscD$^-$ show lower rate constants, indicating a small kinetic isotope effect (KIE), but the pseudo-first-order k_{2D} is not constant with [*i*AscD$^-$]. This deviation is likely due to loss of the deuterium label due to exchange of adventitious water in the MeCN at the lower concentrations of *i*AscD$^-$ (<1 mM).[26] Using data from experiments with higher [*i*AscD$^-$] yields $k_{2H}/k_{2D} = 1.2 \pm 0.1$, which should be taken as the *minimum* KIE since some deuterium is still being lost under these conditions. Attempts were made to ensure high deuterium enrichment by adding millimolar D_2O to the reaction mixtures. However, this results in anomalous kinetic behavior, possibly because the thermodynamics and kinetics of ascorbate reactions are sensitive to the presence of hydrogen bond donors.[24b]

To probe the role of the propionate, the kinetics have also been measured for the reaction of *i*AscH$^-$ with the protonated and methylated iron(III) derivatives, $\mathbf{Fe^{III}{\sim}CO_2H^+}$ and [Fe^{III}(protoporphyrin IX *di*methyl ester)(MeIm)$_2$]OTf [abbreviated $Fe^{III}PPIX_{DME}(MeIm)_2^+$]. Under the same conditions as eq 2, these reactions proceeded only to partial completion based on the optical spectra (Figure 2 and Supporting Information). These observations are consistent with previous studies of PCET reactions between iron-tetraphenyl porphyrin complexes and *i*AscH$^-$.[15] The data for $\mathbf{Fe^{III}{\sim}CO_2H^+}$ + *i*AscH$^-$ can be fit using an approach to equilibrium second-order kinetic model with $k = (2.5 \pm 0.5) \times 10^4$ M^{-1} s^{-1} and an apparent equilibrium constant of 0.13 ± 0.04. This rate constant is a factor of 3 slower than that for $\mathbf{Fe^{III}{\sim}CO_2}$. The data for $Fe^{III}PPIX_{DME}(MeIm)_2^+$ + *i*AscH$^-$ are essentially identical, which is reasonable since the two systems have the same $Fe^{III/II}$ reduction potential (see Supporting Information).

The reactions of $\mathbf{Fe^{III}{\sim}CO_2H^+}$ and $Fe^{III}PPIX_{DME}(MeIm)_2^+$ with *i*AscH$^-$ cannot be simple ET processes. Based on the known redox potentials (Scheme 1 and ref 24a), ET from *i*AscH$^-$ to $\mathbf{Fe^{III}{\sim}CO_2H^+}$ is 0.26 ± 0.02 mV uphill ($K_{ET} = 4 \times 10^{-5}$), inconsistent with the apparent equilibrium constant given above. ET would generate the protonated ascorbyl radical *i*AscH$^{\bullet}$, which is fairly acidic ($pK_a = 14$ in MeCN) and would be mostly deprotonated by the 5 mM MeIm present ($pK_a(HMeIm^+) = 12.2$ in MeCN[27]). Thus these reactions likely occur by *i*AscH$^-$ donating e^- to Fe^{III} and H^+ to MeIm, as shown in eq 3. Consistent with this proposal, increasing the [MeIm] from 0.5 to 10 mM in the reaction of *i*AscH$^-$ + $Fe^{III}PPIX_{DME}(MeIm)_2^+$ shifts the position of equilibrium more toward the products. Assuming mass balance, the optical data indicate an equilibrium constant for reaction 3 of $K_3 = (3 \pm 1) \times 10^{-9}$ ($\Delta G°_3 = 11.6 \pm 0.3$ kcal mol^{-1}) which is in reasonable agreement with the free energy calculated from redox potentials and pK_a values, +10.2 ± 1.2 kcal mol^{-1}. In this case the equilibrium constant is defined by the difference in BDFE of *i*AscH$^-$ and $E_{1/2}(Fe^{III/II}PPIX(MeIm)_2)$ + pK_a(MeIm) + C_G (54.9 kcal mol^{-1}). This is an example of a 'multiple site' or 'separated' PCET/CPET reaction, as discussed in more detail in refs 1c and 3. It should be noted that while MeIm is a strong enough base to deprotonate *i*AscH$^{\bullet}$, it does not deprotonate $\mathbf{Fe^{III}{\sim}CO_2H^+}$ to any significant extent: $pK_a(HMeIm^+) = 12.2$ vs $pK_a(\mathbf{Fe^{III}{\sim}CO_2H^+}) = 21.1$.

$$Fe^{III}PPIX_{DME}(MeIm)_2^+ + i\text{AscH}^- + \text{MeIm} \rightleftharpoons Fe^{II}PPIX_{DME}(MeIm)_2 + i\text{Asc}^{\bullet-} + \text{HMeIm}^+ \quad (3)$$

The reaction of $\mathbf{Fe^{III}{\sim}CO_2}$ with *i*AscH$^-$ (eq 2) does not show this imidazole dependence between 5 and 20 mM MeIm, which indicates that the propionate is acting as the proton acceptor in that case. In addition, the $\mathbf{Fe^{III}{\sim}CO_2}$ + *i*AscH$^-$ reaction is faster than the $\mathbf{Fe^{III}{\sim}CO_2H^+}$ + *i*AscH$^-$ reaction under identical conditions. This is inconsistent with $\mathbf{Fe^{III}{\sim}CO_2}$ + *i*AscH$^-$ proceeding by initial ET since the $\mathbf{Fe^{III}{\sim}CO_2H^+}$ ET reaction is more favorable. These data all support that the propionate is the proton acceptor in the oxidation of *i*AscH$^-$ shown in reaction 2.

2.2.2. Reactions with the Hydroxylamine TEMPOH and Other Hydroxylic Substrates. $\mathbf{Fe^{III}{\sim}CO_2}$ reacts rapidly with an excess of the hydroxylamine TEMPOH (*N*-hydroxy-2,2′-6,6′-tetramethylpiperidine) to give the ferrous porphyrin (by visible spectroscopy) and TEMPO (by EPR, Supporting Information, Figure S14). In the reverse direction, $\mathbf{Fe^{II}{\sim}CO_2H}$ and excess TEMPO also react rapidly, yielding $\mathbf{Fe^{III}{\sim}CO_2}$ and TEMPOH

dx.doi.org/10.1021/ja201663p | J. Am. Chem. Soc. 2011, 133, 8544–8551

(by ^{1}H NMR). Kinetic studies give the forward and reverse rate constants k_4 = 11.4 ± 1.7 M^{-1} s^{-1}, k_{-4} = 4.0 ± 0.5 M^{-1} s^{-1} (Figure 3). The derived equilibrium constant, k_4/k_{-4} = 2.9 ± 0.6, is consistent with that from static UV−vis measurements (3.1 ± 0.6). The agreement between these measurements confirms that $\mathbf{Fe^{II}{\sim}CO_2H}$ is the product of the $\mathbf{Fe^{III}{\sim}CO_2}$ + TEMPOH reaction. The average value of K_4 = 3.0 ± 0.6, together with BDFE(TEMPOH) = 66.5 ± 0.5 kcal mol^{-1},[28] gives BDFE($\mathbf{Fe^{II}{\sim}CO_2H}$) = 67.2 ± 0.5 kcal mol^{-1}, within error of that determined in Scheme 1. Together, these two independent measurements give a consensus BDFE of 67.8 ± 0.6 kcal mol^{-1}. The KIE for D transfer from TEMPOD to $\mathbf{Fe^{III}{\sim}CO_2}$ (k_{4H}/k_{4D}) is 3.9 ± 0.7.

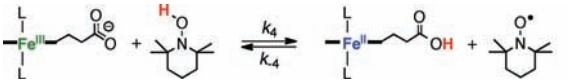

(4)

$\mathbf{Fe^{II}{\sim}CO_2H}$ reacts with the 2,4,6-tri-*tert*-butyl phenoxyl radical (^{t}Bu$_3$ArO$^\bullet$) to give the corresponding phenol by ^{1}H NMR (eq 5). The reaction is quantitative with the stoichiometric phenoxyl radical, consistent with the strong H-abstracting ability of ^{t}Bu$_3$ArO$^\bullet$.[28] $\mathbf{Fe^{II}{\sim}CO_2H}$ reacts similarly with excess benzoquinone to give hydroquinone, and in the reverse direction, $\mathbf{Fe^{III}{\sim}CO_2}$ plus hydroquinone yields benzoquinone (eq 6), with an overall log K_6 = −2.2 ± 0.3. The hydroquinone (H_2Q) reaction K_{eq} and the average BDFE(H_2Q) = 69 ± 2 kcal mol^{-1}[13,15] give BDFE($\mathbf{Fe^{II}{\sim}CO_2H}$) = 67.5 ± 2.0 kcal mol^{-1}, again in excellent agreement with the values derived from Scheme 1 and from equilibration with TEMPO(H).

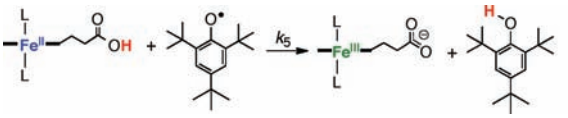

(5)

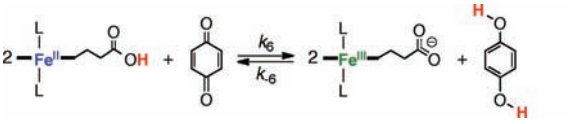

(6)

3. DISCUSSION

The reactions reported here—with ascorbate, TEMPO/TEMPOH, hydroquinone/benzoquinone (H_2Q/Q), and ^{t}Bu$_3$ArO$^\bullet$ (eqs 2, 4, 5, and 6)—all involve net transfers of H$^\bullet$ by the $\mathbf{Fe^{III/II}{\sim}CO_2(H)}$ model complexes (eq 7). $\mathbf{Fe^{II}{\sim}CO_2H}$ is indicated to be the reduced form of the redox couple by

$$\mathbf{Fe^{III}{\sim}CO_2} + \mathbf{H}\text{–}\mathrm{X} \rightarrow \mathbf{Fe^{II}{\sim}CO_2H} + \mathrm{X}^\bullet \qquad (7)$$

stoichiometry, by optical spectroscopy (which indicates the ferrous oxidation state), and by equilibrium measurements with TEMPO/TEMPOH and H_2Q/Q starting either from $\mathbf{Fe^{III}{\sim}CO_2}$ or $\mathbf{Fe^{II}{\sim}CO_2H}$. A key role for the propionate as a proton acceptor is indicated by the thermochemical analysis of the TEMPOH reaction given below, and by the faster and more

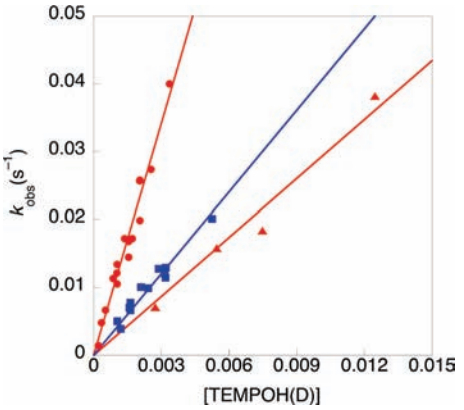

Figure 3. Pseudo-first-order rate constants for $\mathbf{Fe^{III}{\sim}CO_2}$ + TEMPOH (red ●), $\mathbf{Fe^{II}{\sim}CO_2H}$ + TEMPO (blue ■), and $\mathbf{Fe^{III}{\sim}CO_2}$ + TEMPOD (red ▲). The slopes of the lines give the second-order rate constants k_4, k_{-4}, and k_{4D}, respectively.

complete reaction of 5,6-isopropylidene ascorbate (*i*AscH$^-$)with $\mathbf{Fe^{III}{\sim}CO_2}$ versus with its protonated analog $\mathbf{Fe^{III}{\sim}CO_2H^+}$, even though the latter is the stronger one-electron oxidant. The $\mathbf{Fe^{III}{\sim}CO_2}$ + *i*AscH$^-$ reaction is unaffected by the amount of added *N*-methylimidazole (MeIm), while the analogous reactions of $\mathbf{Fe^{III}{\sim}CO_2H^+}$ or $Fe^{III}PPIX_{DME}(MeIm)_2^+$ are affected because MeIm is the proton acceptor. MeIm can deprotonate the *i*AscH$^\bullet$ radical but not $\mathbf{Fe^{III}{\sim}CO_2H^+}$. This variety of evidence for the formation of $\mathbf{Fe^{II}{\sim}CO_2H}$ is important because there is no spectroscopic evidence for a protonated carboxylate in the ferrous product. This difficulty in keeping track of the proton is a common challenge in studies of PCET systems in which the redox and acid/base sites are well separated, or, more generally, when the coupling between the redox and acid/base sites is small (see below).

While these reactions involve the net movement of net H$^\bullet$, they are problematic to describe as hydrogen atom transfer reactions because of the large separation between the iron redox center and the carboxylate proton donor/acceptor. We have argued that HAT reactions are best defined broadly, as the subset of CPET reactions in which $H^+ + e^-$ (H$^\bullet$) are transferred from one donor to one acceptor.[3] This is in contrast to 'multiple-site' CPET reactions such as X−H + base (:B) + oxidant (A+) → X$^\bullet$ + HB$^+$ + A^0, for instance eq 3 above.[1c,3] The reactions that interconvert $\mathbf{Fe^{III}{\sim}CO_2}$ and $\mathbf{Fe^{II}{\sim}CO_2H}$ lie in between these two categories. Our group has previously reported other PCET reactions of this type, involving ruthenium complexes with a distant carboxylate.[25] In the multiple-site reactions, the base and oxidant are completely independent; in $\mathbf{Fe^{II}{\sim}CO_2H}$ there is a small amount of communication between the redox and acid/base sites. This is indicated by the 20 mV shift in the reduction potential upon protonation (equivalently,[3] a 0.3 unit change in the pK_a values for the Fe^{II} and Fe^{III} complexes). As discussed below, many biochemical PCET processes in proteins likely fall in this 'low-coupling' regime, such as redox-driven proton pumps.

3.1. Mechanisms of H^+/e^- Transfer. In principle, all of the PCET reactions described above could occur by proton transfer (PT) and then electron transfer (ET); (ii) ET and then PT; or (iii) concerted transfer of the two particles (CPET). As has been discussed extensively elsewhere, the ground-state energetics of these competing steps can provide powerful mechanistic insight.[29] Thus, the reaction of $\mathbf{Fe^{III}{\sim}CO_2}$ + TEMPOH

dx.doi.org/10.1021/ja201663p |*J. Am. Chem. Soc.* 2011, 133, 8544–8551

(eq 4) cannot occur by initial ET or by initial PT because the $\Delta G°$ for these steps, +32 and +27 kcal mol^{-1}, respectively, are much larger than the observed activation barrier ($\Delta G^{‡}_4$ = 16.0 ± 0.1 kcal mol^{-1}). The $\Delta G°$ values are calculated from the $E°$ and pK_a values of TEMPOH[3] and $\mathbf{Fe^{III}}\sim\mathbf{CO_2H^+}$ (Scheme 1), and $\Delta G^{‡}_4$ is calculated from the k_4 and the Eyring equation. Since the reaction cannot proceed by initial ET or PT, it therefore must occur by concerted transfer of e^- and H^+. This is the first demonstration of a CPET reaction in which a heme-propionate acts as the proton acceptor.

The mechanism of oxidation of ascorbate (eq 2) is not uniquely defined by such thermochemical arguments, but a variety of evidence suggests a CPET pathway. The observed Eyring barrier $\Delta G^{‡}_2$ is +10.5 ± 0.5 kcal mol^{-1}. Using the thermochemical data of *i*AscH$^-$,[30] initial PT to give $\mathbf{Fe^{III}}\sim\mathbf{CO_2H^+}$ and *i*Asc^{2-} has $\Delta G°_{2\text{-PT}}$ = +10.1 ± 0.6 kcal mol^{-1}, and initial ET to give $\mathbf{Fe^{II}}\sim\mathbf{CO_2}^-$ + *i*AscH$^•$ has $\Delta G°_{2\text{-ET}}$ = +6.5 kcal mol^{-1}. Since both of these values are smaller than $\Delta G^{‡}_2$, neither stepwise pathway can be excluded based on these arguments. Still, initial PT is unlikely because the measured barrier is only 0.3 ± 0.6 kcal mol^{-1} below $\Delta G°_{2/\text{PT}}$ and PT reactions in MeCN usually have $\Delta G^{‡}$ significantly greater than $\Delta G°$.[31] Initial rate-limiting ET is also unlikely because reduction of protonated $\mathbf{Fe^{III}}\sim\mathbf{CO_2H^+}$ by *i*AscH$^-$, which is expected to occur by ET, is *ca.* three times slower than k_1 despite being 20 mV more favorable.

3.2. Biochemical Implications and e^-/H^+ Coupling. The oxidation of isopropylidene ascorbate by $\mathbf{Fe^{III}}\sim\mathbf{CO_2}$ (reaction 2) is a model for the substrate-oxidizing step in ascorbate peroxidase (APX, Figure 1). In reaction 2, the ascorbate is oxidized to the radical by transfer of an electron to the iron and a proton to the heme propionate. Ascorbate binds to APX with formation of a hydrogen bond to a propionate, and this is the hydrogen that is lost on oxidation. Therefore we propose that APX follows a similar PCET mechanism, with e^- transfer to the heme-iron and H^+ transfer to the propionate. PPIX-dimethylester substituted APX shows loss of activity,[8b] which is probably due at least in part to the blocking of the proton-accepting site. As noted above, the rate constants for reaction of *i*AscH$^-$ with $\mathbf{Fe^{III}}\sim\mathbf{CO_2H^+}$ or $Fe^{III}PPIX_{DME}(MeIm)_2OTf$ are slower than k_2, consistent with blocking the proton accepting group. The model reaction is not an exact mimic, since the electron is transferred to an Fe^{III} center in the model while the enzymatic oxidant is an Fe^{IV}=O (ferryl) group. The mechanistic data indicate that the model reaction proceeds by concerted proton−electron transfer (CPET). This is also a likely mechanism for APX, although the higher driving force in the enzymatic reaction could allow a stepwise ET/PT pathway.[32]

Propionates have previously been suggested to play important roles in heme-driven proton pumps[4] such as those found in cytochrome oxidase and quinol:fumarate reductase (QFR).[7,10,33] Comparatively fewer reports of propionate involvement in PCET transformations of enzyme substrates have emerged, but a few examples are available. In nitrite reductase, for instance, the hydroquinone substrate appears to bind to the propionate and an axial histidine.[34] This is similar to the model system reaction 6 that interconverts hydroquinone and benzoquinone. Heme propionates may also play a role in proton and electron transfer in the cytochrome b_6f complex, which is responsible for electron transfer between reaction centers in photosynthetic reaction centers. The redox potentials of hemes b_n and x (also known as heme c_i) in this complex are pH dependent,[35] indicating PCET behavior, and the propionate of heme b_n is hydrogen bonded to a water molecule ligated to heme x.[36] Heme x is located near the quinone reduction site, which carries out reactions similar to reaction 6. Nitric oxide synthase (NOS) has a hydrogen bond between the tetrahydrobiopterin (H_4B) cofactor and a heme-propionate, and this H-bond is proposed to play a key role in the catalytic cycle.[37] It has been suggested that electron transfer from H_4B to heme is coupled to proton transfer to the propionate and that the proton is transferred back upon reduction of the pterin. It was proposed that this allows H_4B to mediate $1e^-$ reactions, and not its more common $2e^-$ chemistry.[37] Based on these examples and the model system reported here, we propose that heme propionates may play active roles in PCET reactions in heme proteins, in addition to their structural rules that have long been discussed. Poulos has also commented on the variety of both active and passive roles that heme propionates can play in catalysis, including the effect(s) of the protonation state.[38]

More generally, PCET plays a perhaps underappreciated role in the chemistry of hemes, the quintessential biological redox cofactors. Heme proteins have a range of functions, from redox mediators such as cytochromes c[39] and b_5[40] to oxidation catalysts such as cytochromes P450 and peroxidases.[2] It is well-known that reduction of the ferryl (Fe=O) units in P450s and peroxidases to the resting ferric state requires protons as well as electrons, e.g. $[Fe^{IV}(O)(PPIX^{•+})] \rightarrow Fe^{IV}(OH)(PPIX)$ in P450 and $Fe^{IV}(O)(PPIX) \rightarrow Fe^{III}(OH)(PPIX)$ in peroxidases.[2,41] Cytochrome b_5 is typically described as an electron transfer protein, but its redox potential is pH dependent indicating that proton movement can accompany ET,[40] but neither the propionates nor the vinyl groups appear to be involved.[42] The case for cyt b_5 may be more similar to the ascorbate reductions/oxidations of cyt b_{561} where PCET may occur at an axial histidine/histidinate.

A key issue in these, and all, PCET reactions is the coupling or communication between the proton and the electron. While there are potentially many definitions of this coupling, the simplest and most direct measurement is the *thermodynamic* coupling. For a particular reagent, this is the shift in its pK_a with redox change or the shift in $E°$ with protonation.[3] Expressed in free energy terms, the ΔpK_a and $\Delta E°$ must be exactly the same based on applying Hess' Law to the 'square scheme' thermochemical cycles such as Scheme 1 [$\Delta E° = (RT/F)\Delta pK_a = 0.059$ V × ΔpK_a at 298 K].[3] When the proton is transferred to an atom directly bonded to the redox-active site, as in the ferryl reactions, this coupling can be quite large, >1 V or >17 pK_a units.[43] For the propionate model system described here, where the proton binds to a carboxylate oxygen *seven* bonds removed from the iron, the coupling is very small, $\Delta E°$ = 0.02 V or ΔpK_a = 0.3 (Scheme 1). A small coupling of 0.01 V has been observed in a rigid ruthenium-terpyridyl-benzoate in which the carboxylate oxygens are ten bonds and 11 Å from the Ru center.[25b] The reaction of *i*AscH$^-$ with $\mathbf{Fe^{III}}\sim\mathbf{CO_2}$ proceeds by CPET because of the stronger coupling of the e^- and H^+ in the ascorbate reactant ($\Delta E°$ = 0.7 V/ΔpK_a = 12 for ascorbate in water[3]).

In sum, the coupling of redox and acid/base chemistry—the shift in pK_a upon redox change—is key to many functions of heme cofactors. As noted above, the coupling in ferryls is large, while the coupling is small in proton pumps driven by multiple redox steps with small changes in free energy. The model system described here has a small (20 mV) coupling between the propionate and the iron center. The reactions with ascorbate and TEMPOH occur by concerted proton−electron transfer (CPET) because of the significant coupling of e^- and H^+ in the organic substrate.

4. CONCLUSION

A model heme system has been developed where redox chemistry occurs at iron and acid/base chemistry occurs at a propionate. The model complexes $\mathbf{Fe^{III/II}{\sim}CO_2(H)}$ undergo H-transfer reactions with an ascorbate analog, with TEMPO/TEMPOH, with hydroquinone/benzoquinone and with tri-*tert*-butylphenoxyl. The first two reactions occur via *concerted* proton−electron transfer (CPET), and this is the first demonstration of such reactivity involving a heme-propionate. Heme propionates have long been understood as structural motifs in proteins and have recently been suggested to be involved in redox processes.[44] This study indicates that heme propionate can be directly involved in proton-coupled redox processes and that this possibility should be considered in enzymatic reactions of heme cofactors. The model systems in acetonitrile described here are simpler than the enzymatic environment of a typical heme cofactor, which may include intricate hydrogen bonding networks and/or water channels to bring protons to, or remove them from, the active site. Still, when the substrate is hydrogen bonded directly to the propionate and is thermochemically biased to transfer both a proton and an electron, the results reported here indicate that the heme propionate can be directly involved in CPET. CPET occurs despite the large separation and modest communication between the iron center and the propionate oxygen atoms; this communication or coupling is suggested to be an important parameter in the PCET reactivity of heme cofactors.

5. EXPERIMENTAL SECTION

5.1. General. All solutions for kinetic and equilibrium measurements were prepared in a nitrogen filled glovebox. Synthetic procedures were carried out under air at ambient temperature and pressure. Reagents were purchased from Aldrich, with the exception of DBU (1,8-diazabicyclo-[5.4.0]undec-7-ene, Strem) and hemin chloride (iron(III)protoporphyrin IX chloride, Strem). Hemin was purified according to literature procedures.[45] *N*-Methylimidazole (MeIm) was purified by vacuum distillation and was stored under an inert atmosphere. TEMPOH[21] and ^{t}Bu$_3$PhO$^{\bullet}$[46] were prepared following literature procedures. TEMPOD was synthesized as previously described:[47] enrichment was 98 ± 1% by ^{1}H NMR. *i*AscD$_2$ was prepared by dissolving in CD$_3$OD and removing the solvent under reduced pressure a total of 3 times; enrichment was 98 ± 2% by ^{1}H NMR. Solutions of *i*AscH$^-$ or *i*AscD$^-$ were freshly generated from *i*AscH$_2$ or *i*AscD$_2$ + 1 equiv of DBU.[24] Tetrabutylammonium hexafluorophosphate (^{n}Bu$_4$NPF$_6$) was recrystallized 3 times from absolute ethanol and dried in vacuo for 10 h at 100 °C. DBU was stored in a N$_2$-filled glovebox and used as received. Et$_3$N was freshly distilled from CaH$_2$, degassed, and stored in a N$_2$-filled glovebox. Benzoquinone was purified by vacuum sublimation, and hydroquinone was recrystallized from acetone. Cp$_2$Co (cobaltocene), Cp$_2$Fe (ferrocene), and Cp*$_2$Fe (decamethylferrocene) were purified by vacuum sublimation to a dry ice/acetone coldfinger.

Solvents were purchased from Fischer, and deuterated solvents were purchased from Cambridge Isotope Laboratories. Acetonitrile was used as received from Burdick and Jackson (low water) and was stored in an argon pressurized stainless steel drum, plumbed directly into a glovebox. Methylene chloride, diethyl ether, pentane, toluene, and benzene were dried using a "Grubbs type" Seca Solvent System installed by GlassContour.[48]

^{1}H NMR spectra were obtained on Bruker 300 and 500 MHz spectrometers at 298 K. Chemical shifts are reported in ppm relative to TMS by referencing to residual solvent. EPR spectra were collected at ambient temperature on a Bruker E580 CW/ET EPR spectrometer operating at X-band frequency. Electrospray ionization mass spectra (ESI-MS) were obtained on a Bruker Esquire-LC ion trap mass spectrometer and reported as *m*/*z*. UV/visible spectra were collected at ambient temperature using a Hewlett-Packard 8453 diode array spectrophotometer and are reported as λ_{max} in nm (ε, M^{-1} cm^{-1}). Static UV−vis kinetics were also performed on this instrument with samples thermostatted at 298 K. Cyclic voltammograms were collected using an E2 Epsilon electrochemical analyzer (Bioanalytical Systems); see Supporting Information for full details and cyclic voltammograms.

5.2. Synthesis of Compounds. *5.2.1. Iron(III)protoporphyrin IX Monomethyl Ester Chloride (Fe^{III}(PPIX$_{MME}$)Cl).* Fe^{III}(PPIX$_{MME}$)Cl was synthesized in 34% overall yield by modification of a literature procedure[49] as described in the Supporting Information.

5.2.2. [Fe^{III}(PPIX$_{MME}$)(MeIm)$_2$]OTf (Fe$^{III}{\sim}CO_2H^+$). To a THF (5 mL) solution of Fe^{III}(PPIX$_{MME}$)Cl (0.023 g, 0.035 mmol) was added 91 mg (0.035 mmol) of AgOTf. The solution was stirred under N$_2$ for 3 h followed by filtration through Celite to remove precipitated AgCl. The solvent was removed under reduced pressure, and the resulting solution was redissolved in 5 mL of CH$_2$Cl$_2$ + 15 μL of *N*-methylimidazole. The resulting red solution was stirred for 5 min at room temperature after which Et$_2$O was added to precipitate Fe^{III}(PPIX$_{MME}$)(MeIm)$_2$OTf ($\mathbf{Fe^{III}{\sim}CO_2H^+}$). Yield: 0.031 g (90%). The ^{1}H NMR spectrum was assigned by analogy to Fe^{III}(PPIX)(imidazole)$_2^+$ and Fe^{III}(PPIX-dimethylester)(imidazole)$_2^+$.[50] There are twice as many ^{1}H signals as those for the reference compounds, indicating that $\mathbf{Fe^{III}{\sim}CO_2H^+}$ is a 50/50 mixture of isomers at the 6- and 7-positions. ESI-M: 712 [M − MeIm]$^+$. ^{1}H NMR (CD$_3$CN + 5 mM MeIm, 50/50 mixture of 2 isomers, 500 MHz, Figure S1): δ 19.18 (s, 3H, porp-CH$_3$), 19.08 (s, 3H, porp-CH$_3$), 18.97 (s, 3H, porp-CH$_3$), 18.78 (s, 3H, porp-CH$_3$), 18.10 (br s, 12H, Fe-ImN-CH$_3$), 15.52 (s, 3H, porp-CH$_3$), 15.14 (s, 3H, porp-CH$_3$), 13.11 (m, 1H, α-vinyl), 12.85 (m, 1H, α-vinyl), 12.19 (s, 3H, porp-CH$_3$), 11.81 (m, 1H, α-vinyl), 11.43 (s, 3H, porp-CH$_3$), 11.36 (m, 1H, α-vinyl), 8.87 (br s, 4H, Im-H), 5.88 (s, 1H, porp-H), 5.85 (s, 1H, porp-H), 5.57 (s, 2H, porp-α-CH$_2$), 5.51 (s, 2H, porp-α-CH$_2$), 5.29 (s, 2H, porp-α-CH$_2$), 5.19 (s, 2H, porp-α-CH$_2$), 4.69 (s, 1H, porp-H), 4.66 (s, 1H, porp-H), 3.55 (s, 6H, −CO$_2$CH$_3$), 1.47 (s, 1H, porp-H), 1.44 (s, 1H, porp-H), 1.20 (s, 1H, porp-H), 1.18 (s, 1H, porp-H), 0.93 (s, 8H, porp-β-CH$_2$), −1.35 (d, 1H, vinyl-β-CH), −1.50 (d, 1H, vinyl-β-CH), −1.66 (d, 1H, vinyl-β-CH), −1.83 (s, 1H, vinyl-β-CH), −3.42 (br s, 1H, vinyl-β-CH), −3.45 (br s, 1H, vinyl-β-CH), −3.79 (m, 2H, vinyl-β-CH), −4.42 (br s, 1H, Im-H) ppm. One of the imidazole-CH resonances was not observed; it could be attributed to the very broad signal around 13 ppm or be obscured by the other resonances. Anal. Calcd for C$_{44}$H$_{46}$F$_3$FeN$_8$O$_7$S: C, 55.99; H, 4.91; N, 11.87. Found: C, 55.64; H, 4.87; N, 11.87.

5.2.3. Characterization of Fe^{II}PPIX$_{MME}$(MeIm)$_2$ Species (Fe$^{II}{\sim}CO_2H$ and Fe$^{II}{\sim}CO_2^-$). $\mathbf{Fe^{II}{\sim}CO_2H}$ was generated by addition of 1 equiv of Cp$_2$Co to MeCN solutions of isolated $\mathbf{Fe^{III}{\sim}CO_2H^+}$ in the presence of 5 mM MeIm. Additions of more than 1 equiv of Cp$_2$Co caused no further UV−vis spectral changes, indicating 1 e^- reduction of the ferric species. The starting complex could be regenerated cleanly with 1 equiv of tri(*p*-tolyl)aminium (tol$_3$N$^{\bullet+}$) oxidant. UV−vis (MeCN), Q-bands 528 (14 000), 558 (27 000). The λ_{max} and ε are in agreement with model complexes[51] and with ferrous cytochrome b_5 (bis(histidine) ligated).[52]

The deprotonated compound $\mathbf{Fe^{II}{\sim}CO_2^-}$ is indistinguishable from $\mathbf{Fe^{II}{\sim}CO_2H}$ by UV−vis spectroscopy. Addition of up to 5 equiv of DBU causes no change in the Soret or Q-bands. Based on the pK_a calculated from the difference in redox potentials (see text), 1 equiv of DBU should fully deprotonate $\mathbf{Fe^{II}{\sim}CO_2H}$.

5.2.4. Characterization of Deprotonated Fe^{III}PPIX$_{MME}$(MeIm)$_2$ (Fe$^{III}{\sim}CO_2$). $\mathbf{Fe^{III}{\sim}CO_2}$ was generated by addition of 1 equiv of either DBU (pK_a = 24.3[53]) or ^{n}Bu$_4$NOH (1 M in MeOH) to MeCN solutions of isolated $\mathbf{Fe^{III}{\sim}CO_2H^+}$ in the presence of 5 mM MeIm. This follows previous reports that addition of a stoichiometric base to

bis(imidazole)-ligated hemes in the presence of excess imidazole gives six-coordinate complexes, without displacement of imidazole by the base.[54] Generation of $\mathbf{Fe^{III}{\sim}CO_2}$ can be done by working quickly with static UV, or more conveniently with stopped-flow UV−vis, as described below. Addition of up to 1 equiv of excess base caused no further UV−vis spectral changes. The addition of 1 equiv of triflic acid to solutions of $\mathbf{Fe^{III}{\sim}CO_2}$ cleanly regenerates $\mathbf{Fe^{III}{\sim}CO_2H^+}$. The spectra show no dependence on [MeIm] up to 20 mM (the highest concentration tested). UV−vis (MeCN), Q-bands 535 (7700), 616 (3800).

5.3. Stopped-Flow Kinetics. All kinetics experiments were carried out as previously described.[15,24,25] Full details are given in the Supporting Information.

5.4. Kinetic and Equilibrium Measurements by Stopped-Flow. The determination of the pK_a of $\mathbf{Fe^{III}{\sim}CO_2H^+}$, confirmation of the redox $\mathbf{Fe^{III/II}{\sim}CO_2H}$ and $\mathbf{Fe^{III/II}{\sim}CO_2^-}$ redox potentials by equilibration with Cp^*_2Fe, and all of the kinetic studies were done using an OLIS RSM-1000 stopped-flow rapid-scanning spectrophotometer. In a typical procedure, a solution of $\mathbf{Fe^{III}{\sim}CO_2}$, 0.1 ^{n}Bu$_4NPF_6$, and 5 mM MeIm in MeCN was freshly generated from $\mathbf{Fe^{III}{\sim}CO_2H^+}$ and 1 equiv of DBU and then was loaded into one syringe. The other syringe was loaded with a similar solution of 10−45 equiv of *i*AscH$^-$ in MeCN/0.1 ^{n}Bu$_4$NPF$_6$/5 mM MeIm. The kinetic data were analyzed using a first-order model. Experimental details and plots are given in the Supporting Information.

■ ASSOCIATED CONTENT

Supporting Information. ^{1}H NMR spectrum of Fe^{III}(PPIX$_{MME}$)(MeIm)$_2$OTf, cyclic voltammograms of iron complexes, pK_a and redox titration data, stopped-flow kinetics data, EPR spectra. This material is available free of charge via the Internet at http://pubs.acs.org.

■ AUTHOR INFORMATION

Corresponding Author
jwarren@caltech.edu; mayer@chem.washington.edu

■ ACKNOWLEDGMENT

We gratefully acknowledge financial support from the U.S. National Institutes of Health (1F32GM095037 to J.J.W. and GM50422 to J.M.M.) and the University of Washington. We thank Dr. Stefan Ochsenbein for help obtaining EPR spectra.

■ REFERENCES

(1) (a) Stubbe, J.; Nocera, D. G.; Yee, C S.; Chang, M. C. Y. *Chem. Rev.* **2003**, *103*, 2167–2201. (b) Mayer, J. M. *Annu. Rev. Phys. Chem.* **2004**, *55*, 363–390. (c) Huynh, M. H. V.; Meyer, T. J. *Chem. Rev.* **2007**, *107*, 5004–5064.

(2) (a) Dunford, H. B. *Heme Peroxidases*; Wiley-VCH: New York, 1999. (b) *Cytochrome P450: Structure, Mechanism and Biochemistry*, 3rd ed.; Ortiz de Montellano, P. R., Ed.; Kluwer Academic/Plenum: New York, 2005. (c) Rittle, J.; Green, M. T. *Science* **2010**, *330*, 933−937 and references therein.

(3) Warren, J. J.; Tronic, T. A.; Mayer, J. M. *Chem. Rev.* **2010**, *110*, 6961–7001.

(4) (a) Nakanishi, N.; Rahman, M. M.; Sakamoto, Y.; Miura, M.; Takeuchi, F.; Park, S.-Y.; Tsubaki, M. *J. Biochem.* **2009**, *146*, 857–866. (b) Njus, D.; Wigle, M.; Kelley, P. M.; Kipp, B. H.; Schlegel, H. B. *Biochemistry* **2001**, *40*, 11905–11911. (c) Nakanishi, N.; Takeuchi, F.; Tsubaki, M. *J. Biochem.* **2007**, *142*, 553–560.

(5) CPET (coined in: Costentin, C.; Evans, D. H.; Robert, M.; Savéant, J.-M. *J. Am. Chem. Soc.* **2005**, *127*, 12490–12491) implies transfer of e^- and H^+ in the same kinetic step, while PCET refers to any process affected by transfer of both electron(s) and proton(s).

(6) (a) Bertero, M. G.; Rothery, R. A.; Boroumand, N.; Palak, M.; Blasco, F.; Ginet, N.; Weiner, J. H.; Strynadka, N. C. J. *J. Biol. Chem.* **2005**, *280*, 14836–14843. (b) Crane, B. R.; Arvai, A. S.; Ghosh, D. K.; Wu, C.; Getzoff, E. D.; Stuehr, D. J.; Tainer, J. A. *Science* **1998**, *279*, 2121–2126. (c) Brzezinski, P.; Ädelroth, P. *Curr. Opin. Struct. Biol.* **2006**, *16*, 465–472.

(7) (a) Haas, A. H.; Sauer, U. S.; Gross, R.; Simon, J.; Mäntele, W.; Lancaster, C. R. D. *Biochemistry* **2005**, *44*, 13949–13961. (b) Lancaster, C. R. D.; Sauer, U. S.; Groβ, R.; Haas, A. H.; Graf, J.; Schwalbe, H.; Mäntele, W.; Simon, J.; Madej, M. G. *Proc. Natl. Acad. Sci. U.S.A.* **2005**, *102*, 18860–18865.

(8) (a) Sharp, K. H; Mewies, M.; Moody, P. C. E.; Raven, E. L. *Nat. Struct. Biol.* **2003**, *10*, 303–307. (b) Macdonald, I. K.; Badyal, S. K.; Ghamsari, L.; Moody, P. C. E.; Raven, E. L. *Biochemistry* **2006**, *45*, 7808–7817.

(9) See, for instance: Guallar, V. *J. Phys. Chem. B* **2008**, *112*, 13460–13464.

(10) (a) Kaila, V. R. I.; Verkhovsky, M. I.; Wikström, M. *Chem. Rev.* **2010**, *110*, 7062–7081. (b) See also: Chang, H.-Y.; Hemp, J.; Chen, Y.; Fee, J. A.; Gennis, R. B. *Proc. Natl. Acad. Sci. U.S.A.* **2009**, *106*, 16169–16173.

(11) (a) Das, D. K.; Medhi, O. K. *J. Inorg. Biochem.* **1998**, *70*, 83–90. (b) Das, D. K.; Medhi, O. K. *Indian J. Chem., Sect. A: Inorg., Bio-inorg., Phys., Theor. Anal. Chem.* **2005**, *44A*, 2228–2232.

(12) Generated using the PyMOL Molecular Graphics System, Version 1.2r3pre, Schrödinger, LLC.

(13) (a) Rosenthal, J.; Hodgkiss, J. M.; Young, E. R.; Nocera, D. G. *J. Am. Chem. Soc.* **2006**, *128*, 10474–10483. (b) Young, E. R.; Rosenthal, J.; Hodgkiss, J. M.; Nocera, D. G. *J. Am. Chem. Soc.* **2009**, *131*, 7678–7684. (c) Cukier, R. I.; Nocera, D. G. *Annu. Rev. Phys. Chem.* **1998**, *49*, 337–369. (d) Hodgkiss, J. M.; Rosenthal, J.; Nocera, D. G. In *Hydrogen-Transfer Reactions*; Hynes, J. T., Klinman, J. P., Limbach, H.-H., Schowen, R. L., Eds.; Wiley-VCH: Weinheim, Germany, 2007; Vol. 2.17, pp 503−561. (e) Pressé, S.; Silbey, R. *J. Chem. Phys.* **2006**, *124*, 164504–164511.

(14) For related Fe(PPIX) complexes, see: Little, R. G.; Dymock, K. R.; Ibers, J. A. *J. Am. Chem. Soc.* **1975**, *97*, 4532–4539.

(15) Warren, J. J.; Mayer, J. M. *J. Am. Chem. Soc.* **2008**, *130*, 2774–2776.

(16) Asakura, T.; Lamson, D. W. *Anal. Biochem.* **1973**, *53*, 448–451.

(17) The large difference between the Q-bands of $\mathbf{Fe^{III}{\sim}CO_2H^+}$ and $\mathbf{Fe^{III}{\sim}CO_2}$ is surprising. Similar changes are observed on adding 1 equiv of DBU to the bis(N-MeIm) complex of native PPIX (not esterified).

(18) Pagola, S.; Stephens, P. W.; Bohle, D. S.; Kosar, A. D.; Madsen, S. K. *Nature* **2000**, *404*, 307–310.

(19) Stynes, D. V.; Fletcher, D.; Chen, X. *Inorg. Chem.* **1986**, *25*, 3483–3488.

(20) Reid, L. S.; Taniguchi, V. T.; Gray, H. B.; Mauk, A. G. *J. Am. Chem. Soc.* **1982**, *104*, 7516–7519.

(21) C_G = 54.9 kcal mol^{-1} in MeCN versus $Cp_2Fe^{+/0}$. Mader, E. A.; Davidson, E. R.; Mayer, J. M. *J. Am. Chem. Soc.* **2007**, *129*, 5153–5166.

(22) (a) De Santis, G.; Fabbrizzi, L.; Licchelli, M.; Pallaviicini, P. *Inorg. Chim. Acta* **1994**, *225*, 239–244. (b) Herres-Pawlis, S.; Verma, P.; Haase, R.; Kang, P.; Lyons, C. T.; Wasinger, E. C.; Flörke, U.; Henkel, G.; Stack, T. D. P. *J. Am. Chem. Soc.* **2009**, *131*, 1151–1169.

(23) (a) Waidmann, C. R. PhD. Thesis, University of Washington, Seattle, WA, October 2009. (b) Reference 3, Section 5.9.

(24) (a) Warren, J. J.; Mayer, J. M. *J. Am. Chem. Soc.* **2008**, *130*, 7546–7547. (b) Warren, J. J.; Mayer, J. M. *J. Am. Chem. Soc.* **2010**, *132*, 7784–7793.

(25) (a) Manner, V. W.; Dipasquale, A. G.; Mayer, J. M. *J. Am. Chem. Soc.* **2008**, *130*, 7210–7211. (b) Manner, V. W.; Mayer, J. M. *J. Am. Chem. Soc.* **2009**, *131*, 9874–9875.

(26) Karl Fischer titration shows that the minimum water content is 6×10^{-4} M, roughly the same concentration as that of *i*AscD$^-$ used in this study.

(27) Kozak, A.; Czaja, M.; Chmurzyński, L. *J. Chem. Thermodynamics* **2006**, *38*, 599–605.
(28) 66.5 ± 0.5 kcal mol^{-1}. Mader, E. A.; Manner, V. W.; Markle, T. F.; Wu, A.; Franz, J. A.; Mayer, J. M. *J. Am. Chem. Soc.* **2009**, *131*, 4335–4345.
(29) See, for instance, refs 1b, 1c, 3, 4, 15, and 25.
(30) $E_{1/2}(i\text{AscH}^{\bullet/-}) = -0.41$ V versus $Cp_2Fe^{+/0}$ and $pK_a(i\text{AscH}^-) = 28.7$.[3]
(31) (a) Brzezinski, B.; Schroeder, G.; Jarczewski, A.; Grech, E.; Mowicka-Scheibe, J.; Stefaniak, L.; Klimkiewicz, J. *J. Mol. Struct.* **1996**, *377*, 149–154. (b) Schroeder, G.; Brzezinski, B.; Jarczewski, A.; Grech, E.; Milart, P. *J. Mol. Struct.* **1996**, *384*, 127–133. (c) Schroeder, G.; Brezinski, B.; Podebski, D.; Grech, E. *J. Mol. Struct.* **1997**, *416*, 11–19. (d) Grzeskowiak, I.; Galezowski, W.; Jarczewski, A. *Can. J. Chem.* **2001**, *79*, 1128–1134.
(32) (a) Reference 32b shows the favoring of stepwise paths at higher overall driving force. Reference 32c gives the reduction potential of compounds I and II in APX, but it is not known whether these are pure ET potentials or if they also involve proton(s). (b) Sjödin, M.; Irebo, T.; Utas, J. E.; Lind, J.; Merényi, G.; Åkermark, B.; Hammarström, L. *J. Am. Chem. Soc.* **2006**, *128*, 13076–13083. (c) Efimov, I.; Papadopoulou, N. D.; McLean, K. J.; Badyal, S. K.; Macdonald, I. K.; Munro, A. W.; Moody, P. E. C.; Raven, E. L. *Biochemistry* **2007**, *46*, 8017–8023.
(33) Hammes-Schiffer, S.; Stuchebrukhov, A. A. *Chem. Rev.* **2010**, *110*, 6939–6960.
(34) (a) Magalon, A.; Lemesle-Meunier, D.; Rothery, R. A.; Frixon, C.; Weiner, J. H.; Blasco, F. *J. Biol. Chem.* **1997**, *272*, 25652–25658. (b) Lanciano, P.; Magalon, A.; Bertrand, P.; Guigliarelli, B.; Grimaldi, S. *Biochemistry* **2007**, *46*, 5323–5329. (c) Grimaldi, S.; Arias-Cartin, R.; Lanciano, P.; Lyubenova, S.; Endeward, B.; Prisner, T. F.; Magalon, A.; Guigliarelli, B. *J. Biol. Chem.* **2010**, *285*, 179–187.
(35) Alric, J.; Pierre, Y.; Picot, D.; Lavergne, J.; Rappaport, F. *Proc. Natl. Acad. Sci. U.S.A.* **2005**, *102*, 15860–15865.
(36) Kurisu, G.; Zhang, H.; Smith, J. L.; Cramer, W. A. *Science* **2003**, *302*, 1009–1014.
(37) Stoll, S.; NejatyJahromy, Y.; Woodward, J. J.; Ozarowski, A.; Marletta, M. A.; Britt, R. D. *J. Am. Chem. Soc.* **2010**, *132*, 11812–11823.
(38) Poulos, T. L. *Nat. Prod. Rep.* **2007**, *24*, 504–510.
(39) Millet, F. In *Cytochrome c: A Multidisciplinary Approach*; Scott, R. A., Mauk, A. G., Eds.; University Science: Sausalito, CA, 1996; pp 475−487.
(40) Reid, L. S.; Taniguchi, V. T.; Gray, H. B.; Mauk, A. G. *J. Am. Chem. Soc.* **1982**, *104*, 7516–7519.
(41) (a) Green, M. T. *Curr. Opin. Chem. Biol.* **2009**, *13*, 84–88. (b) Rittle, J.; Green, M. T. *Science* **2010**, *330*, 933–937.
(42) (a) Reid, L. S.; Taniguchi, V. T.; Gray, H. B.; Mauk, A. G. *J. Am. Chem. Soc.* **1982**, *104*, 7516–7519. (b) Reid, L. S.; Mauk, M. R.; Mauk, A. G. *J. Am. Chem. Soc.* **1984**, *106*, 2182–2185. (c) Reid, L. S.; Lim, A. R.; Mauk, A. G. *J. Am. Chem. Soc.* **1986**, *108*, 8197–8201.
(43) For example: (a) For $[(bpy)_2(py)Ru(O/H)]^{2+}$, $\Delta E° > 1.1$ V;[43b] for *trans*-$[Ru^V(tmc)(O)(O/H)]^{2+}$, $\Delta E° > 1.2$ V (tmc = tetramethylcyclam);[43c] for $TpCl_2Os(NPhH/H)$, $\Delta E° = 1.53$ V, $\Delta pK_a = 25.5$ (Tp = hydrotrispyrazolylborate).[43d] (b) Lebeau, E. L.; Binstead, R. A.; Meyer, T. J. *J. Am. Chem. Soc.* **2001**, *123*, 10535. (c) Lam, W. W. Y.; Man, W.-L.; Leung, C.-F.; Wong, C.-Y.; Lau, T.-C. *J. Am. Chem. Soc.* **2007**, *129*, 13646. (d) Soper, J. D.; Mayer, J. M. *J. Am. Chem. Soc.* **2003**, *125*, 12217.
(44) Guallar, V.; Olsen, B. *J. Inorg. Biochem.* **2006**, *100*, 755–760. See also ref 9, 10 and 38.
(45) Armarego, W. L. E.; Chai, C. L. L. *Purification of Laboratory Chemicals*, 5th ed.; Butterworth−Heinemann: Amsterdam, 2003.
(46) Manner, V. W.; Markle, T. F.; Freudenthal, J.; Roth, J. P.; Mayer, J. M. *Chem. Commun.* **2008**, 256–258.
(47) Wu, A.; Mader, E. A.; Hrovat, D. A.; Borden, W. T.; Mayer, J. M. *J. Am. Chem. Soc.* **2009**, *131*, 11985–11997.
(48) http://www.glasscontour.com.
(49) Asakura, T.; Lamson, D. W. *Anal. Biochem.* **1973**, *53*, 448–451.
(50) La Mar, G.; Walker, F. A. In *The Porphyrins*; Dolphin, D., Ed.; Academic: New York, 1979; Vol. 4, Part B, pp 61−157; see especially p 76.
(51) Stynes, D. V.; Fletcher, D.; Chen, X. *Inorg. Chem.* **1986**, *25*, 3483–3488.
(52) Reid, L. S.; Taniguchi, V. T.; Gray, H. B.; Mauk, A. G. *J. Am. Chem. Soc.* **1982**, *104*, 7516–7519.
(53) Kaljurand, I.; Kütt, A.; Sooväli, L.; Rodima, T.; Mäemets, V.; Leito, I.; Koppel, I. A. *J. Org. Chem.* **2005**, *70*, 1019–1028.
(54) (a) Quinn, R.; Nappa, M.; Valentine, J. S. *J. Am. Chem. Soc.* **1982**, *104*, 2588–2595. (b) Chacko, V. P.; La Mar, G. N. *J. Am. Chem. Soc.* **1982**, *104*, 7002–7007.